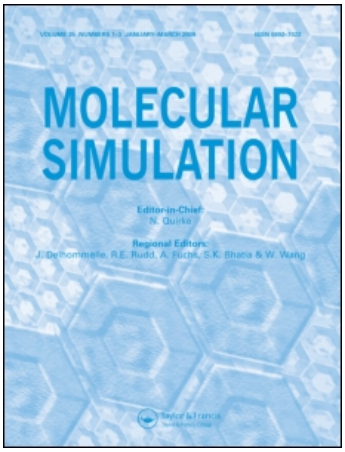

Molecular Simulation
Publication details, including instructions for authors and subscription information:
http://www.informaworld.com/smpp/title~content=t713644482

Simulating the vapour-liquid equilibria of 1,4-dioxane

A. O. Yazaydin[a]; R. W. Thompson[a]
[a] Department of Chemical Engineering, Worcester Polytechnic Institute, Worcester, MA, USA

To cite this Article Yazaydin, A. O. and Thompson, R. W.(2006) 'Simulating the vapour-liquid equilibria of 1,4-dioxane', Molecular Simulation, 32: 8, 657 — 662
To link to this Article: DOI: 10.1080/08927020600883277
URL: http://dx.doi.org/10.1080/08927020600883277

Molecular Simulation, Vol. 32, No. 8, 15 July 2006, 657–662

Taylor & Francis
Taylor & Francis Group

Simulating the vapour–liquid equilibria of 1,4-dioxane

A. O. YAZAYDIN and R. W. THOMPSON*

Department of Chemical Engineering, Worcester Polytechnic Institute, 100 Institute Road, Worcester, MA 01609, USA

(Received March 2006; in final form June 2006)

1,4-dioxane, a cyclic ether, is an emerging contaminant which is difficult to remove from water with conventional water treatment methods and resistant to biodegradation. Once a reliable force field is developed for 1,4-dioxane, molecular simulation techniques can be useful to study alternative adsorbents for its removal. For this purpose, we carried out Monte Carlo simulations in a constant volume Gibbs Ensemble to generate a force field which is capable of predicting the vapour–liquid coexistence curve and critical data of 1,4-dioxane. Results are given in comparison with experimental data and results from simulations with other force fields. Liquid densities and critical temperature are predicted in excellent agreement with experimental data using the new force field. At high temperatures, predicted vapour densities are in good agreement with experimental data, however, at lower temperatures the predicted vapour densities deviate about an order of magnitude from the experimental values. The critical density is slightly underestimated with our new force field. However, overall, the results of simulations with the new parameters give much better agreement with experimental data compared to the results obtained using other force fields.

Keywords: Cyclic ether; Molecular simulation; Phase equilibria; Force field

1. Introduction

1,4-dioxane is a cyclic ether and listed as one of the emerging contaminants by US Environmental Protection Agency (EPA). By emerging, it is meant that it has not until recently been seen as a chemical of concern for the EPA's remedial action programs [1]. Even short exposure to high levels of 1,4-dioxane has caused vertigo and irritation of the eyes, nose, throat, lungs and skin in humans [2,3]. Rats and mice exposed to 1,4-dioxane in their drinking water developed liver carcinomas and adenomas and nasal cavity squamous cell carcinomas [4]. As a result the, EPA has classified 1,4-dioxane as a Group B2, probable human carcinogen [5].

1,4-dioxane is a large production chemical, used as a stabilizer for chlorinated solvents, and during the manufacture of polyester and various polyethoxylated compounds it is formed as a by-product. Improper disposal of industrial wastes and accidental solvent spills have resulted in the contamination of groundwater with 1,4-dioxane [6]. Carbon adsorption and air stripping do not remove 1,4-dioxane efficiently from water due to the fact that 1,4-dioxane is infinitely soluble in water and has a low vapour pressure. The boiling point of 1,4-dioxane (bp = 101°C) makes distillation extremely costly [7]. Due to its high resistance to biotransformation conventional biological processes fail as effective means of treatment [8,9]. Advanced oxidation technologies, utilizing hydrogen peroxide, ozone, and/or UV photo oxidation, are the only processes proven to reduce 1,4-dioxane in substantial amounts, however, they are not cost effective [10,11].

We are interested in simulating the adsorption of 1,4-dioxane in nanoporous materials, since other remediation technologies appear to be ineffective. However, in order to do that, reliable parameters are required. To our knowledge a force field has not been developed specifically for 1,4-dioxane or cyclic ethers although 1,4-dioxane and tetrahydrofuran are industrially important solvents. There are a few molecular simulation studies in the literature about 1,4-dioxane, but they are all liquid 1,4-dioxane simulations [12–15]. When simulating fluids in nanoporous materials it is important to have a force field which is capable of predicting the phase equilibria and critical data of the fluid of interest, since fluids may undergo a phase transition when they are confined in nanoporous materials [16]. In this study, we present our work on developing a force field for 1,4-dioxane, which is capable of estimating

*Corresponding author. Email: rwt@wpi.edu

Molecular Simulation
ISSN 0892-7022 print/ISSN 1029-0435 online © 2006 Taylor & Francis
http://www.tandf.co.uk/journals
DOI: 10.1080/08927020600883277

Table 1. Non-bonded force field parameters used in this study.

	New force field		*Trappe-UA**		*OPLS-UA*[†]		*Geerlings*[‡]		*Krienke*[¶]	
	O	CH_2	*O*	CH_2	*O*	CH_2	*O*	CH_2	*O*	CH_2
σ(Å)	2.80	3.85	2.80	3.95	3.07	3.905	3.07	3.905	3.0	3.80
ε/k_B(K)	98.0	51.3	55.0	46.0	85.55	59.38	85.55	59.38	85.5	59.4
$q(e)$	−0.5	0.25	−0.5	0.25	−0.5	0.25	−0.35	0.175	−0.46	0.23

* Refs. [18–21]. † Ref. [17]. ‡ Ref. [14]. ¶ Ref. [15].

its phase equilibria and critical point data. We also present the results of Configurational Bias Monte Carlo (CBMC) simulations using this new force field in comparison with available experimental data and the results of simulations performed with other force fields.

2. Model and simulation details

We used a pairwise-additive potential in the form of 12-6 Lennard-Jones (LJ) plus columbic potential to compute the site–site non-bonded interactions:

$$V_{ij} = 4\varepsilon_{ij}\left[\left(\frac{\sigma_{ij}}{r_{ij}}\right)^{12} - \left(\frac{\sigma_{ij}}{r_{ij}}\right)^{6}\right] + \frac{q_i q_j}{4\varepsilon_0 r_{ij}}.$$

where i and j are methylene and oxygen sites of 1,4-dioxane, and r_{ij} is the distance between sites i and j. ε_{ij} and σ_{ij} are LJ well depth and diameter, respectively. q_i and q_j are the partial charges of the interacting sites. To maintain the bonds and bending angles flexible a simple harmonic potential was used for both terms

$$V_{\text{bond}} = k_r(r - r_0).$$

$$V_{\text{bend}} = k_\theta(\theta - \theta_0).$$

where r, r_0, k_r are the measured bond length, the equilibrium bond length, and the bond force constant, respectively; and θ, θ_0, k_θ are the measured bending angle, the equilibrium bending angle, and the bending force constant, respectively. A cosine series was employed for torsional interactions of sites separated by three bonds

$$V_{\text{tors}} = c_0 + c_1[1 + \cos(\phi)] + c_2[1 - \cos(2\phi)] + c_3[1 + \cos(3\phi)]$$

where ϕ and c_i are the dihedral angle and the i_{th} coefficient, respectively. 1–4 non-bonded interactions within the same molecule were scaled by a factor of 0.5 in addition to the torsional potential.

To compare our force field with others we performed simulations using the non-bonded parameters developed for ethers in OPLS-UA [17], and Trappe-UA [18–21] force fields, and using the non-bonded parameters from the works of Geerlings *et al.* [14] and Krienke *et al.* [15] where they simulated 1,4-dioxane in its liquid state (table 1). All force fields mentioned here model the methylene group as a united atom. In the new force field partial charges for oxygen and methylene sites were taken from OPLS-UA force field. These partial charges are also used by the Trappe-UA force field and very close to the values derived from the quantum mechanical calculations [15]. Lorentz–Berthelot (LB) mixing rules, given by

$$\varepsilon_{ij} = \sqrt{\varepsilon_{ii}\varepsilon_{jj}} \quad \text{and} \quad \sigma_{ij} = \frac{\sigma_{ii} + \sigma_{jj}}{2}$$

were used to calculate the non-bonded pair interactions in our new force field, as is the case in the work of Krienke *et al.* [15] and in the Trappe-UA force field. OPLS-UA force field, on the other hand, uses geometric mixing rules.

$$\varepsilon_{ij} = \sqrt{\varepsilon_{ii}\varepsilon_{jj}} \quad \text{and} \quad \sigma_{ij} = \sqrt{\sigma_{ii}\sigma_{jj}}.$$

The mixing rule used by Geerlings *et al.* [14] is a complex one which is a function of the polarizability of the interacting sites. They mentioned setting the polarizabilities of oxygen and methylene to the polarizabilities of water and methane, repectively; however, they neither reported the resulting values nor cited any reference for the polarizabilities. The only thing they reported was that they used the LJ parameters of OPLS-UA force field and after the mixing rule was applied the resulting values between unlike sites were slightly different from those obtained from geometric mixing rules. Therefore, we decided to use geometric mixing rules for the LJ parameters of Geerlings *et al.* [14].

We used a single set of intramolecular potential in all our simulations regardless of the source of non-bonded terms, since each of these force fields we found in literature treat intramolecular terms differently (table 2). The bonding parameters used for ether oxygen and carbon

Table 2. Parameters for intramolecular terms.

Bonding		
	CH_2–CH_2	O–CH_2
k_{bond}/k_B (K)	155997.15	161029.32
r_0 (Å)	1.54	1.41
Angle bending		
	CH_2–CH_2–O	CH_2–O–CH_2
k_{bend}/k_B (K)	25150	30200
θ_0 (°)	112.0	112.0
Torsion		
	O–CH_2–CH_2–O	CH_2–CH_2–O–CH_2
c_0/k_B (K)	503.24	0.0
c_1/k_B (K)	0.0	725.35
c_2/k_B (K)	−251.62	−163.75
c_3/k_B (K)	1006.47	558.20

atoms in the Amber [22] force field were used to maintain flexible bonds in our simulations. Angle bending and $CH_2-CH_2-O-CH_2$ torsion parameters were taken from the OPLS-UA force field. $O-CH_2-CH_2-O$ torsion parameters were taken from the Amber force field.

All simulations were performed using the *Towhee* [23] Monte Carlo code and in the constant volume version of the Gibbs ensemble [24–26]. A total number of 180 molecules were used in two boxes in which two phases were formed eventually. Periodic boundary conditions were applied in all directions. The Ewald sum method was employed to calculate the electrostatic interactions. A cut-off distance of 10 Å was used. Simulations were performed within a range of temperatures from 298.15 to 525 K. Simulations were run for 20,000 cycles to equilibrate the system, followed by a 20,000-cycle production run. A cycle is equal to N Monte Carlo moves, where N is the number of molecules in the system. Statistical uncertainties were calculated by dividing the production run into 20 blocks.

Cyclic molecules are quite difficult to grow using standard CBMC methods, because the probability of closing a ring structure during the growth process is almost zero. Additional biasing is required during the growth procedure in order to encourage the growth to form reasonable ring closures. Therefore, in addition to the standard Coupled–Decoupled CBMC [19] method that *Towhee* employs, a Fixed Endpoint CBMC [27,28] method also was used.

Some analytical biasing functions are used in this method. These functions transform the distance between growth atoms and target ring atoms consistently, into a bias function which depends loosely on dihedral, bending and vibrational energies.

We optimized the LJ parameters of oxygen and methylene for our new force field by systematically modifying them to predict the vapour–liquid coexistence curve (VLCC) and the critical data of 1,4-dioxane satisfactorily. We started this optimization procedure by taking oxygen LJ parameters of Trappe-UA and methylene LJ parameters of Fox *et al.* [38]. The critical temperatures (T_c) and densities (ρ_c) were calculated using the saturated density scaling law [29,30] and the law of rectilinear diameters with a scaling exponent of $\beta = 0.3047$ [31]. After the LJ parameters were optimized we investigated the finite size effects by carrying out the simulations with 300 molecules.

The Monte Carlo moves consisted of volume changes of boxes between each other, swap moves between two boxes, regrowths of the molecules, intramolecular single atom translation, translation of the centre-of-mass, and rotation about the centre-of-mass with corresponding probabilities of 3, 25, 5, 7, 30, 30%, respectively. All simulations were performed on *64-bit AMD Opteron, 2.4 GhZ* cpus. A typical simulation involving 180 molecules took 5 h per 10,000 cycles.

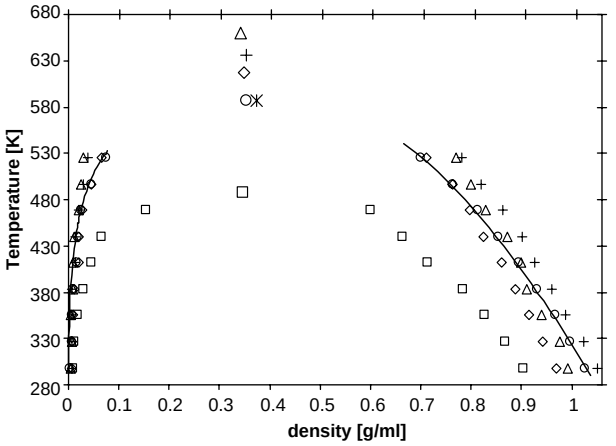

Figure 1. VLCC for 1,4-dioxane. New force field (○), Trappe-UA (□), OPLS-UA (Δ),Geerlings (◇) [14], Krienke (+) [15], Experimental critical data (*). Solid lines represent the experimental liquid densities [31] and vapour densities calculated from the experimental vapour pressure [33] using Pitzer's [34] method.

3. Results and discussion

The VLCC, critical temperature, and density of 1,4-dioxane are given in figure 1, along with the results of our simulations using our new force field, as well as the predictions using the parameters from Trappe-UA and OPLS-UA force fields, and from the works of Geerlings *et al.* [14], and Kerienke *et al.* [15]. Our new force field gives excellent agreement with experimental liquid densities while the liquid densities calculated using the parameters from other force fields showed different degrees of deviation. Liquid densities predicted by using the OPLS-UA force field underestimate the experimental data in the low temperature region, but then overestimate as the temperature increases. The parameters of Geerlings *et al.* [14] yielded similar behaviour at lower temperatures by underestimating the liquid densities; however, at higher temperatures predictions were more successful. Results obtained using the parameters of Krienke *et al.* [15] overestimate the experimental liquid densities. In the case of the Trappe-UA force field, results deviated significantly from the experimental data by underestimating them. The Trappe-UA force field is specifically parameterized for estimating phase equilibria and the results of ordinary ether molecules simulated by Trappe-UA reproduces experimental data quite successfully [21]. However, it is

Table 3. Comparison of the critical density and temperature obtained from experiments and simulations with the new force field. The subscripts denote the statistical uncertainties in the last digit(s) where available.

T_c (K)		ρ_c (g/ml)	
Simulation	*Experimental*	*Simulation*	*Experimental*
587_{23}	585.15*, 588†, 588.15‡, 587.3¶, 587§	0.354_{24}	0.360329*, 0.37018§

* Ref. [32]. † Ref. [35]. ‡ Ref. [36]. ¶ Ref. [37]. § Ref. [31].

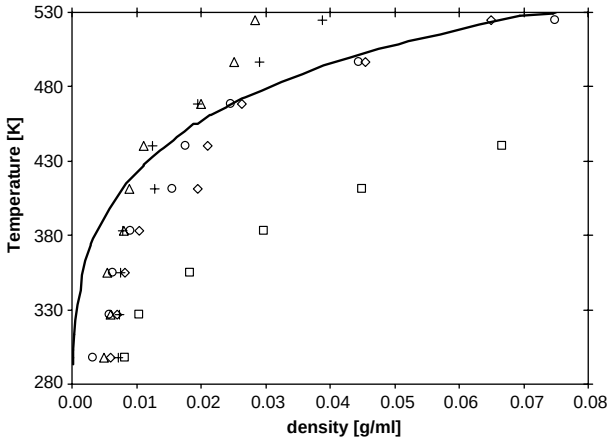

Figure 2. A magnified view of the vapour densities. New force field (○), Trappe-UA (□), OPLS-UA (Δ),Geerlings (◇) [14], Krienke (+) [15]. Solid line represent the vapour densities calculated from the experimental vapour pressures [33] using Pitzer's [34] method.

interesting to see that when a cyclic ether is modelled with the same parameters the differences can be rather large.

The critical temperature estimated with our new force field is also in excellent agreement with the experimental critical temperature data (table 3). On the other hand, the critical temperature estimated using the parameters of OPLS-UA, Geerlings *et al.* [14], and Krienke *et al.* [15] overestimate, and Trappe-UA force field underestimate the critical temperature. The critical density is slightly underestimated with our force field, but still gives good agreement with experimental data, particularly with the value given in [32] (table 2). When compared to the critical density estimated using parameters from other sources our force field gives better agreement with the experimental critical density.

To our knowledge experimental vapour densities of 1,4-dioxane are not available in the literature, so we estimated them using experimental vapour pressures [33] and the method of Pitzer *et al.* [34]. A magnified view of the vapour densities section of figure 1 is given in figure 2. The predicted vapour densities using the Trappe-UA force field underestimate the vapour densities computed from experimental vapour pressure. When the parameters of OPLS-UA force field and Krineke *et al.* [15] were used, the experimental values were underestimated at lower temperatures, and as the temperature increases the true values are overestimated. Vapour densities predicted using the new force field, and the parameters of Geerlings *et al.* [14] are in good agreement above 430 K, but below this temperature deviation from the experimental values is around an order of magnitude. This deviation at lower temperatures results in slight underestimation of the critical density. However, compared to other force fields, the new force field gives the best agreement for vapour densities. A similar phenomenon was also observed in several cyclic alkanes, especially in cyclohexane, cyclopentane, [40] and linear alkanes [18].

To study the low temperature vapour phase configuration in detail and bring an explanation to the high predicted vapour densities we computed the radial distribution functions [39] of O–O, CH_2–O, CH_2–CH_2 pairs of 1,4-dioxane in the vapour phase at 298.15 K (figure 3). In all three cases there is a peak around 5 Å, which indicates the possibility of dimers in the vapour phase. When we visually examined the vapour phase configuration snapshots from the simulation we also observed that some 1,4-dioxane molecules were close to each other, although most molecules were far away from each other. These dimers present may be a factor in the resulting high vapour densities at lower temperatures. The deviation of predicted vapour densities from the experimental data can be due to other reasons, including the inadequate representation of cyclic molecules with the united-atom approach and the use of LJ function [41].

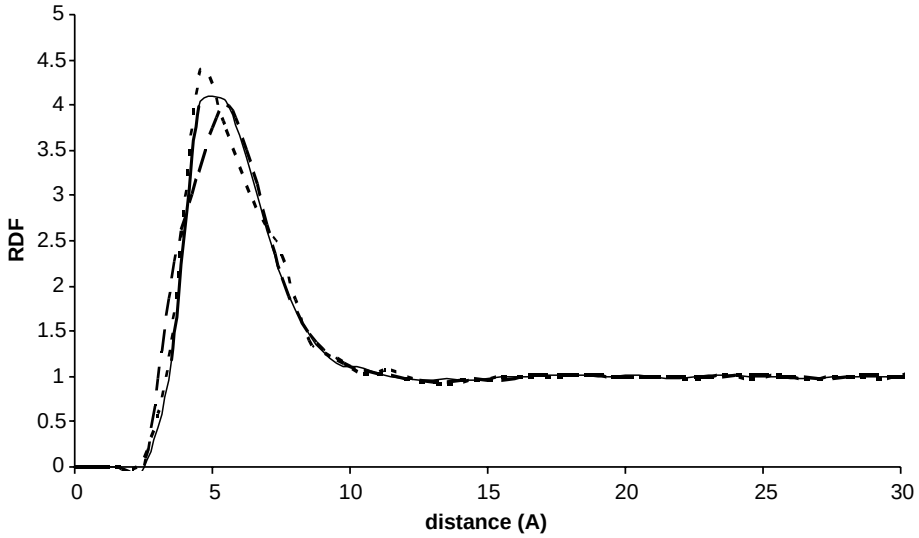

Figure 3. Radial distribution functions of O—O (- - - -), CH_2—O (– – –), CH_2—CH_2 (—) pairs of 1,4-dioxane molecule in the vapour phase at 298.15 K.

Table 4. Compressibility factors calculated from experimental vapour pressure data and those computed from simulations with new force field. The subscripts denote the statistical uncertainties in the last digit(s) where available.

Temperature (K)	*Experimental*	*Simulation*
298.15	0.994	0.944_{22}
326.51	0.986	0.917_{29}
354.86	0.974	0.929_{51}
383.22	0.950	0.924_{66}
411.58	0.928	0.882_{95}
439.93	0.894	0.897_{78}
468.29	0.854	0.863_{56}
496.64	0.785	0.798_{69}
525.0	0.703	0.716_{57}

We calculated the compressibility factors of 1,4-dioxane at nine different temperatures with the new force field (table 4). Up to about 400 K 1,4-dioxane behaves very much like an ideal gas, but then gradually deviates from this behaviour. After this point, the compressibility factors we computed were in good agreement with the values derived from experimental vapour pressures.

To investigate the finite size effects we computed liquid and vapour densities by carrying out the simulations with 300 molecules. The agreement between the densities computed with 180 and 300 molecules is quite convincing (figures 4 and 5), especially the liquid densities give a perfect match. These results provide strong evidence that liquid and vapour densities of 1,4-dioxane computed using our force field parameters are not sensitive to the number of molecules, at least beyond 180.

Finally, we computed the heat of vaporization of 1,4-dioxane at room temperature and at its boiling temperature by using the vapour pressure approach which is fully described elsewhere [42]. The heat of vaporization of 1,4-dioxane at room temperature and at its boiling point was computed to be 37.19_{73} and 32.65_{93} kJ/mol, respectively. These values are close to the reported experimental values, which are 38.4 and 34.2 kJ/mol [43] at the room temperature and at 1,4-dioxane's boiling point, respectively.

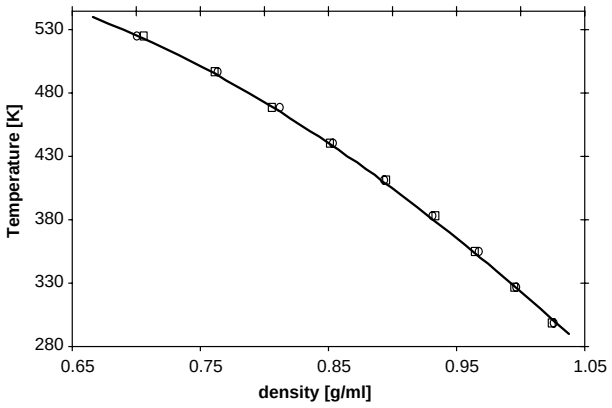

Figure 4. Liquid densities of 1,4-dioxane. New force field 180 molecules (○), New force field 300 molecules (□). Solid line represent the experimental liquid densities [31].

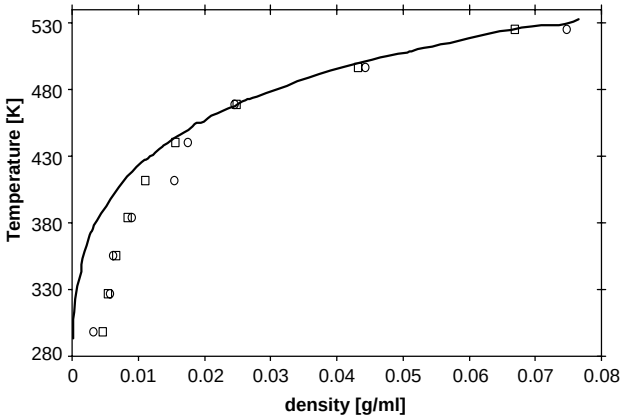

Figure 5. Vapour densities of 1,4-dioxane. New force field 180 molecules (○), New force field 300 molecules (□). Solid lines represent the vapour densities calculated from the experimental vapour pressures [33] using Pitzer's [34] method.

4. Conclusions

We have developed a new force field for 1,4-dioxane, an important industrial solvent which has emerged as a potentially significant threat to human health. Predictions of experimental critical point data and phase behaviour with our new force field outperformed predictions from simulations with other force field parameters available in literature. Liquid densities and the critical temperature were estimated in almost perfect agreement with corresponding experimental data. The critical density was only slightly underestimated with our new force field. At high temperatures, vapour densities also were predicted satisfactorily, however, at lower temperatures where 1,4-dioxane behaves like an ideal gas, deviations up to an order of magnitude were observed. Computed heats of vaporization at room temperature and at its boiling point are close to the experimental values.

The primary objective of this study was to develop reliable atom-atom interaction parameters to use in the simulation of the adsorption of 1,4-dioxane in different adsorbent materials. We validated our new parameters by predicting the experimental phase behaviour, critical temperature, and the critical density. The successful results give us confidence to use the new parameters in our further studies.

Acknowledgements

The authors acknowledge the support of the National Science Foundation through the NSF NIRT award DMI-0210258. Technical help on computing platforms from Josh Brandt, WPI Computing and Communications Center, Senior UNIX Systems Administrator, is gratefully acknowledged.

References

[1] US Environmental Protection Agency, Measurement and monitoring technologies for the 21st century. *17th Quarterly Literature Search*, October 17 (2005).

[2] E.J. Calabrese, E.M. Kenyon. *Air Toxics and Risk Assessment*, Lewis Publishers, Chelsea, MI (1991).

[3] S. Budavari (Ed.). *The Merck Index, An Encyclopedia of Chemicals, Drugs, and Biologicals*, 11th ed., Merck and Co. Inc., Rahway, NJ (1989).

[4] National Cancer Institute (NCI), Bioassay of 1,4-dioxane for possible carcinogenicity. (1978), CAS No. 123-91-1. NCI Carcinogenesis Technical Report Series No. 80. NCI-CG-TR80. National Institutes of Health, Bethesda, MD

[5] U.S. Environmental Protection Agency, *Integrated Risk Information System (IRIS) on 1,4-Dioxane*, National Center for Environmental Assessment, Office of Research and Development, Washington, DC (1999).

[6] M.J. Zenker, R.C. Borden, M.A. Barlaz. Occurrence and treatment of 1,4-dioxane in aqueous environments. *Environ. Eng. Sci.*, **20**, 423 (2003).

[7] J.H. Suha, M. Mohsenib. A study on the relationship between biodegradability enhancement and oxidation of 1,4-dioxane using ozone and hydrogen peroxide. *Water Res.*, **38**, 2596 (2004).

[8] C.D. Adams, P.A. Scanlan, N.D. Secrist. Oxidation and biodegradability enhancement of 1,4-dioxane using hydrogen peroxide and ozone. *Environ. Sci. Technol.*, **28**, 1812 (1994).

[9] S.L. Kelley, E.W. Aitchison, M. Deshpande, J.L. Schnoor, P.J.J. Alvarez. Biodegradation of 1,4-dioxane in planted and unplanted soil: effect of bioaugmentation with *Amycolata* sp. CB1190. *Water Res.*, **35**, 3791 (2001).

[10] J.C. Alonso, J.C. Johnson, P.J. Linton. 1,4-Dioxane—history, regulatory issues, and the potential remedial impacts. *16th Annual International Conference on Contaminated Soils, Sediments, and Water*, Amherst, MA (2000).

[11] T.K.G. Mohr. *Solvent Stabilizers: White Paper*, Santa Clara Valley Water District, San Jose, CA (2001).

[12] M. Luhmer, M.L. Stien, J. Reisse. Relative polarity of 1,3-dioxane and 1,4-dioxane studied by the reaction field-theory and via computer-simulations. *Heterocycles*, **37**, 1041 (1994).

[13] M. Luhmer, J. Reisse. Molecular dynamics simulations study of NMR relaxation of xenon-133 dissolved in 1,3-dioxane and 1,4-dioxane. *J. Chem. Phys.*, **98**, 1566 (1993).

[14] J.D. Geerlings, C.A.G.O. Varma, M.C. van Hemert. Molecular dynamics studies of a dipole in liquid dioxanes. *J. Phys. Chem. B*, **104**, 56 (2000).

[15] H. Krienke, G. Ahn-Ercan, J. Barthel. Alkali metal halide solutions in 1,4-dioxane-water mixtures. A Monte Carlo simulation study. *J. Mol. Liq.*, **109**, 115 (2004).

[16] A. Giaya, R.W. Thompson. Water confined in cylindrical micropores. *J. Chem. Phys.*, **117**, 3464 (2002).

[17] J.M. Briggs, T. Matsui, W.L. Jorgensen. Monte Carlo simulations of liquid alkyl ethers with the OPLS potential functions. *J. Comput. Chem.*, **11**, 958 (1990).

[18] M.G. Martin, J.I. Siepmann. Transferable potentials for phase equilibria. 1. United-atom description of *n*-alkanes. *J. Phys. Chem. B*, **102**, 2569 (1998).

[19] M.G. Martin, J.I. Siepmann. Novel configurational-bias Monte Carlo method for branched molecules. Transferable potentials for phase equilibria. 2. United-atom description of branched alkanes. *J. Phys. Chem. B*, **103**, 4508 (1999).

[20] B. Chen, J.J. Potoff, J.I. Siepmann. Monte Carlo calculations for alcohols and their mixtures with alkanes. Transferable potentials for phase equilibria. 5. United-atom description of primary, secondary and tertiary alcohols. *J. Phys. Chem. B*, **105**, 3093 (2001).

[21] J.M. Stubbs, J.J. Potoff, J.I. Siepmann. Transferable potentials for phase equilibria. 6. United-atom description for ethers, glycols, ketones and aldehydes. *J. Phys. Chem. B*, **108**, 17596 (2004).

[22] W.D. Cornell, P. Cieplak, C.I. Bayly, I.R. Gould, K.M. Merz Jr., D.M. Ferguson, D.C. Spellmeyer, T. Fox, J.W. Caldwell, P.A. Kollman. A second generation force field for the simulation of proteins, Nucleic acids, and organic molecules. *J. Am. Chem. Soc.*, **117**, 5179 (1995).

[23] http://towhee.sourceforge.net

[24] A.Z. Panagiotopoulos. Direct determination of phase coexistence properties of fluids by Monte Carlo simulation in a new ensemble. *Mol. Phys.*, **61**, 813 (1987).

[25] A.Z. Panagiotopoulos, N. Quirke, M. Stapleton, D.J. Tildesley. Phase equilibria by simulation in the Gibbs ensemble. Alternative derivation, generalization, and application to mixture and membrane equilibria. *Mol. Phys.*, **63**, 527 (1988).

[26] B. Smit, P.H. Desmedt, D. Frenkel. Computer simulations in the Gibbs ensemble. *Mol. Phys.*, **68**, 931 (1989).

[27] M.G. Martin, A.P. Thompson. Industrial property prediction using Towhee and LAMMPS. *Fluid Phase Equilib.*, **217**, 105 (2004).

[28] M.G. Martin, A.L. Frischknecht. Using arbitrary trial distributions to improve intramolecular sampling in configurational-bias Monte Carlo. *Mol. Phys.* (in press).

[29] J.S. Rowlinson, B. Widom. *Molecular Theory of Capillarity*, Oxford University Press, New York (1989).

[30] J.S. Rowlinson, F.L. Swinton. *Liquids and Liquid Mixtures*, 3rd ed., Butterworths, London (1982).

[31] C.L. Yaws. *Yaws' Handbook of Thermodynamic and Physical Properties of Chemical Compounds*, Knovel, Norwich, NY (2003).

[32] K. Hojendahl. Dielectric constant, viscosity, surface tension, and critical data of boron tribromide, dioxane, and ethylene dichloride. *Mat.-fys. Medd.-K. Danske Vidensk. Selsk.*, **24**, 1 (1946).

[33] C.G. Vinson Jr., J.J. Martin. Heat of vaporization and vapour pressure of 1,4-dioxane. *J. Chem. Eng. Data*, **8**, 74 (1963).

[34] K.S. Pitzer, D.Z. Kippman, R.F. Curl Jr., C.M. Huggins, E. Petersen. The volumetric and thermodynamic properties of fluids. II. Compressibility factor, vapor pressure and entropy of vaporization. *J. Am. Chem. Soc.*, **77**, 3433 (1955).

[35] K.A. Kobe, A.E. Ravicz, S.P. Vohra. Critical properties and vapour pressures of some ethers and heterocyclic compounds. *Ind. Eng. Chem.*, **1**, 50 (1956).

[36] F. Glaser, H. Ruland. Untersuchungsen über dampfdruckkurven und kritische daten einiger technisch wichtiger organischer substanzen. *Chem. Ing. Techn.*, **29**, 772 (1957).

[37] G. Cristou, C.L. Young, P. Svejda. Gas-liquid critical temperatures of mixtures of propane, butane, pentane, sulfur hexafluoride, dichlorodifluoromethane and chlorotrifluoromethane with less volatile compounds of a range of varying polarities. *Fluid Phase Equilib.*, **67**, 45 (1991).

[38] J.P. Fox, V. Rooy, S.P. Bates. Simulating the adsorption of linear, branched and cyclic alkanes in silicalite-1 and $AlPO_4$-5. *Microporous Mesoporous Mater.*, **69**, 9 (2004).

[39] M.P. Allen, D.J. Tildesley. *Simulation of Liquids*, Clarendon Press, Oxford (1989).

[40] J.S. Lee, C.D. Wick, J.M. Stubbs, J. Siepmann. Simulating the vapor−liquid equilibria of large cyclic alkanes. *Mol. Phys.*, **103**, 99 (2005).

[41] B. Chen, M.G. Martin, J.I. Siepmann. Thermodynamic properties of the Williams, OPLS-AA, and MMFF94 all-atom force fields for normal alkanes. *J. Phys. Chem. B*, **102**, 2578 (1998).

[42] M.G. Martin, M.J. Biddy. Monte Carlo simulation predictions for the heat of vaporization of acetone and butyramide. *Fluid Phase Equilib.*, **236**, 53 (2005).

[43] J.A. Dean (Ed.). *Lange's Handbook of Chemistry*, McGraw-Hill, New York (1999).